Materials Physics and Mechanics 17 (2013) 142-157 Received: August 28, 2013

INFLUENCE OF IMPERFECT INTERFACE ON REFLECTION AND TRANSMISSION COEFFICIENTS OF PLANE WAVES BETWEEN TWO DIFFERENT FLUID SATURATED POROUS HALF SPACES

Rajneesh Kumar[1], Aseem Meglani[2], Sanjay Garg[3*]

[1]Department of Mathematics, Kurukshetra University, Kurukshetra, Haryana, India

[2]Department of Mathematics, Chaudhary Devilal University, Sirsa, Haryana, India

[3]Department of Mathematics, R.K.S.D. (P.G.) College Kaithal, Haryana, India

*e-mail: sanjaygarg_153@yahoo.com

Abstract. The present study is concerned with the reflection and transmission of plane waves at an imperfect interface between two different fluid saturated porous half spaces. The expression for the reflection and transmission coefficients which are the ratios of the amplitude of reflected and transmitted waves to the amplitude of incident waves are obtained for an imperfect boundary and deduced for normal stiffness, transverse stiffness. The variations of amplitude ratios with angle of incidence are depicted graphically. A particular case of reflection at the free surface in fluid saturated porous half spaces has been deduced and discussed. A special case of interest has also been deduced from the present investigation. It is found that amplitude ratios of the reflected and transmitted waves are affected by the stiffness of the media.

1. Introduction

The dynamic response of porous media is of great interest in various areas such as geophysics, soil-mechanics, civil engineering, petroleum engineering and environmental engineering. As most of the modem engineering structures are generally made up of multiphase porous continuum, the classical theory, which represents a fluid saturated porous medium as a single phase material, is inadequate to represent the mechanical behavior of such materials especially when the pores are filled with liquid. In this context the solid and liquid phases have different motions. Due to these different motions and different material properties and the complicated geometry of pore structures; the mechanical behavior of a fluid saturated porous medium is very complex and difficult. So from time to time, researchers have tried to overcome this difficulty and considerable work has been done in this regard.

Based on the work of von Terzaghi [1, 2], Biot [3] proposed a general theory of three-dimensional consolidation. Taking the compressibility of the soil into consideration, the water contained in the pores was taken to be incompressible. Biot [4, 5] developed the theory for the propagation of stress waves in porous elastic solids containing a compressible viscous fluid and demonstrated the existence of two types of compressional waves (a fast and a slow wave) along with one shear wave. Biot's model was broadly accepted and some of his results have been taken as standard references and the basis for subsequent analysis in acoustic, geophysics and other such fields.

Based on the work of Fillunger model [6] (which is further based on the concept of volume fractions combined with surface porosity coefficients), Bowen [7] and De Boer and

$$\boldsymbol{E}_S = \frac{1}{2}\,(\text{grad}\ \boldsymbol{u}_S + \text{grad}^{\,T}\ \boldsymbol{u}_S), \tag{5}$$

where $u_i, \dot{u}_i, \ddot{u}_i$ i = F,S denote the displacement, velocities and acceleration of fluid and solid phases respectively and p is the effective pore pressure of the incompressible pore fluid; ρ^s and ρ^F are the densities of the solid and fluid respectively; $\boldsymbol{T}_E{}^{\boldsymbol{S}}$ is the stress in the solid phase and $\boldsymbol{E}_S$ is the linearized langrangian strain tensor; λ^s and μ^s are the macroscopic Lame's parameters of the porous solid and η^s and η^F are the volume fractions satisfying $\eta^s + \eta^F = 1$.

The case of isotropic permeability, the tensor S_V describing the coupled interaction between the solid and fluid is given by De Boer and Ehlers [9], as

$$\mathbf{S}_V = \frac{(\eta^F)^2 \gamma^{FR}}{K^F}\mathbf{I},$$

where γ^{FR} is the effective specific weight of the fluid and K^F is the Darcy's permeabilitbility coefficient of the porous medium.

3. Formulation of the problem

We consider two fluid saturated incompressible porous half spaces being in contact with each other at the plane surface which we designate as plane z = 0 of rectangular Cartesian coordinate system OXYZ. The Z- axis is taken downward pointing into the medium.

For two dimensional problem, we assume the displacement vector $\boldsymbol{u}_i$ (i=F, S) as

$$\boldsymbol{u}_i = (u^i, 0, w^i), \text{ where } \ i=F,S. \tag{6}$$

Using equation (6) in equations (1) - (3) we obtain the following equations for fluid saturated incompressible porous medium as:

$$(\lambda^S + \mu^S)\frac{\partial \theta^S}{\partial x} + \mu^S \nabla^2 u^S - \eta^S \frac{\partial p}{\partial x} - \rho^S \frac{\partial^2 u^S}{\partial t^2} + S_V\left[\frac{\partial u^F}{\partial t} - \frac{\partial u^S}{\partial t}\right] = 0, \tag{7}$$

$$(\lambda^S + \mu^S)\frac{\partial \theta^s}{\partial z} + \mu^S \nabla^2 w^S - \eta^S \frac{\partial p}{\partial z} - \rho^S \frac{\partial^2 w^S}{\partial t^2} + S_V\left[\frac{\partial w^F}{\partial t} - \frac{\partial w^s}{\partial t}\right] = 0, \tag{8}$$

$$\eta^F \frac{\partial p}{\partial x} + \rho^F \frac{\partial^2 u^F}{\partial t^2} + S_V\left[\frac{\partial u^F}{\partial t} - \frac{\partial u^S}{\partial t}\right] = 0, \tag{9}$$

$$\eta^F \frac{\partial p}{\partial z} + \rho^F \frac{\partial^2 w^F}{\partial t^2} + S_V\left[\frac{\partial w^F}{\partial t} - \frac{\partial w^s}{\partial t}\right] = 0, \tag{10}$$

$$\eta^S\left[\frac{\partial^2 u^S}{\partial x \partial t} + \frac{\partial^2 w^S}{\partial z \partial t}\right] + \eta^F\left[\frac{\partial^2 u^F}{\partial x \partial t} + \frac{\partial^2 w^F}{\partial z \partial t}\right] = 0, \tag{11}$$

where $\theta^S = \frac{\partial (u^S)}{\partial x} + \frac{\partial (w^S)}{\partial z}$.

We define the dimensionless quantities defined as:

$$x' = \frac{\omega^*}{C_1} x\,,\ z' = \frac{\omega^*}{C_1} z\,,\ t' = \omega^* t\,,\ u'^S = \left[\frac{\lambda^S + 2\mu^S}{E}\right]\frac{\omega^*}{C_1} u^S\,,\ w'^s = \left[\frac{\lambda^S + 2\mu^S}{E}\right]\frac{\omega^*}{C_1}\ w^S\,,$$

$$u'^F = \left[\frac{\lambda^S + 2\mu^S}{E}\right]\frac{\omega^*}{C_1} u^F\,,\ w'^F = \left[\frac{\lambda^S + 2\mu^S}{E}\right]\frac{\omega*}{C_1}\ w^F\,,\ p' = \frac{p}{E}\,,\ T_{31}{}' = \frac{T_{31}}{E}\,,\ T_{33}{}' = \frac{T_{33}}{E}\ ,$$

$$K_n' = \frac{C_1}{\lambda^S\ \omega^*} K_n\,,\ K_t' = \frac{C_1}{\lambda^S\ \omega^*} K_t\,. \tag{12}$$

In these relations E is the Young's modulus of the solid phase, ω^* is a constant having the dimensions of frequency, C_1 is the velocity of a longitudinal wave propagating in a fluid saturated incompressible porous medium and is given by

$$C_1 = \sqrt{\frac{(\eta^F)^2(\lambda^S + 2\mu^S)}{(\eta^F)^2\rho^S + (\eta^S)^2\rho^F}}\,, \tag{13}$$

If pore is absent or gas is filled in the pores then ρ^F is very small as compare to ρ^S and can be neglected so the relation reduce to

$$C_0 = \sqrt{\frac{\lambda^S + 2\mu^S}{\rho^S}}\,. \tag{14}$$

This gives the velocity of the longitudinal wave propagating in an incompressible empty porous solid where the change in volume is due to the change in porosity and well known result of the classical theory of elasticity .In an incompressible non porous solid $\eta^F \to 0$, then (13) becomes $C_1 = 0$ and physically acceptable as longitudinal wave cannot propagate in an incompressible medium.

The displacement components u^i and w^i are related to the non dimensional potential ϕ^i and ψ^i as

$$u^i = \frac{\partial\phi^i}{\partial x} + \frac{\partial\psi^i}{\partial z}\,,\ w^i = \frac{\partial\phi^i}{\partial z} - \frac{\partial\psi^i}{\partial x}\,. \quad \text{i = F, S.} \tag{15}$$

Making use of non dimensional quantities given by (12) in equations (7) – (11) and with the help of (15) we obtain the following equations determining φ^S, φ^F, p, ψ^S, ψ^F as:

$$\nabla^2\phi^S - \frac{\partial^2\phi^S}{\partial t^2} - \frac{\delta_2}{(\eta^F)^2}\frac{\partial\phi^S}{\partial t} = 0, \tag{16}$$

$$\phi^F = -\frac{\eta^S}{\eta^F}\ \phi^S\,, \tag{17}$$

$$(\eta^F)^2\,\mathrm{p} - \eta^S\delta_1^{\,2}\frac{\rho^F}{\rho^S}\frac{\partial^2\phi^S}{\partial t^2} - \delta_2\frac{\partial\phi^S}{\partial t} = 0, \tag{18}$$

$$\delta^2\nabla^2\psi^S - \delta_1^{\,2}\frac{\partial^2\psi^S}{\partial t^2} + \delta_2\left[\frac{\partial\psi^F}{\partial t} - \frac{\partial\psi^S}{\partial t}\right] = 0, \tag{19}$$

$$\delta_1^{\,2}\,\frac{\rho^F}{\rho^S}\,\frac{\partial^2\psi^F}{\partial t^2}+\delta_2\left[\frac{\partial\psi^F}{\partial t}-\frac{\partial\psi^S}{\partial t}\right]=0, \tag{20}$$

where $\delta_1=\dfrac{C_1}{C_O}$, $\delta=\dfrac{\beta_0}{C_O}$, $\beta_O=\sqrt{\dfrac{\mu^S}{\rho^S}}$, $\delta_2=\dfrac{S_V C_1^{\,2}}{w^*\rho^S C_O^{\,2}}$.

4. Reflection and transmission of the waves

We consider a plane waves propagating through a medium M_1 which we designate as the region Z > 0 and incident at the plane z = 0 and making an angle θ_0 with normal to the surface. Corresponding to each incident wave (longitudinal / transverse wave) we get two reflected waves in the medium M_1 and two transmitted waves in medium M_2. We write all the variables without bar in the region Z > 0 (medium M_1) and attach a bar to denote the variables in the region $Z<0$ (medium M_2) as shown in the Fig. 1 (Geometry of the problem).

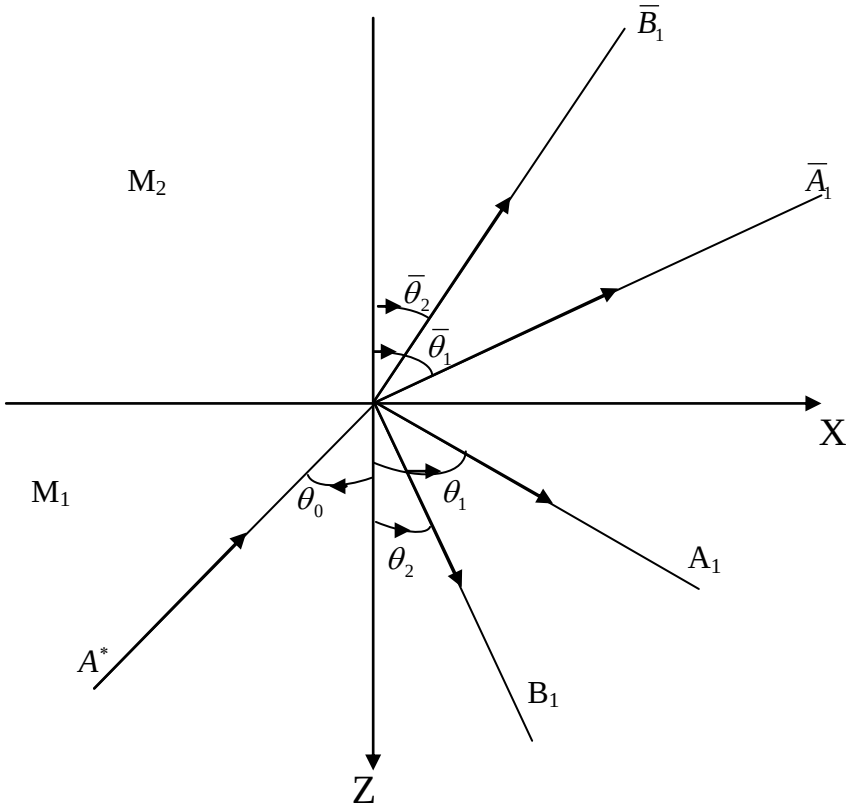

Fig. 1. Geometry of the problem.

We assume the solution of the system of equations (16) - (20) in the form

$$(\phi^S,\phi^F,\psi^S,\psi^F,\text{p}) = (\phi_1^{\,S},\phi_1^{\,F},\psi_1^{\,S},\psi_1^{\,F},p_1\quad)\exp[\text{i k (x sin }\theta\text{ - z cos}\theta\text{) – i}\omega\text{ t]}, \tag{21}$$

where k is the wave number and ω is the complex circular frequency.
Making the use of (21) in equations (16), (19) - (20) we obtain two quadric equations in V given by

$$V^2 + AV + B = 0, \tag{22}$$

$V^2 + CV + D = 0,$ (23)

where A = $\frac{i\delta_2}{k(\eta^F)^2}$, B = -1, C = $\frac{\delta_2}{k\delta_1^{\,2}}\left[i + \frac{\delta_2\rho^S}{\delta_1^{\,2}\rho^F\omega + i\delta_2\rho^S}\right]$, D = $-\frac{\delta^2}{\delta_1^{\,2}}$.

The velocities of the longitudinal waves are the roots of equation (22):

$$V_1 = \frac{-A \pm \sqrt{A^2 - 4B}}{2},$$

and the velocities of the transverse waves are the roots of equation (23):

$$V_2 = \frac{-C \pm \sqrt{C^2 - 4D}}{2},$$

where the upper sign correspond to the incident wave and lower sign correspond to the reflected wave.

5. Boundary conditions

We have considered two fluid saturated incompressible porous half spaces .Imperfect bounding considered here mean that the traction is continuous across the interface but the small displacements are assumed to depend linearly on the traction vector.

Boundary conditions at the interface z = 0 are:

$\bar{T}_{33}^{\,S} = \mathrm{K_n}(w^S - \bar{w}^S),$ (24)

$(\bar{T}_{31}^{\,S}) = \mathrm{K_t}(u^S - \bar{u}^S),$ (25)

$(T_{33}^{\,S} - p) = (\bar{T}_{33}^{\,S} - \bar{p}),$ (26)

$(T_{31}^{\,S}) = (\bar{T}_{31}^{\,S}),$ (27)

where K_n, K_t denote normal and transverse stiffness of layer having dimension N/m^3.

In view of (21) we assume the values of $\phi^S, \phi^F, \psi^S, \psi^F$ and p satisfying the boundary conditions for medium M_1 and M_2 as:

Medium M_1:

$\{\phi^S, \phi^F, p\} = \{1, m_1, m_2\}[A_{01} \exp\{i k_1 (x \sin\theta_0 - z \cos\theta_0) - i\omega_1 t\} + A_1 \exp\{i k_1 (x \sin\theta_1 + z \cos\theta_1) - i\omega_1 t\}],$ (28)

$\{\psi^S, \psi^F\} = \{1, m_3\}[B_{01} \exp\{i k_2 (x \sin\theta_0 - z \cos\theta_0) - i\omega_2 t\} + B_1 \exp\{i k_2 (x \sin\theta_2 + z \cos\theta_2) - i\omega_2 t\}].$ (29)

Medium M_2:

$\{\bar{\phi}^S, \bar{\phi}^F, \bar{p}\} = \{1, \bar{m}_1, \bar{m}_2\}[\bar{A}_1 \exp\{i\bar{k}_1 (x \sin\bar{\theta}_1 - z \cos\bar{\theta}_1) - i\bar{\omega}_1 t\}],$ (30)

$\{\psi^S, \psi^F\} = \{1, \bar{m}_3\}[\bar{B}_1 \exp\{i\bar{k}_2 (x \sin\bar{\theta}_2 - z \cos\bar{\theta}_2) - i\bar{\omega}_2 t\}],$ (31)

where

$m_1 = -\frac{\eta^S}{\eta^F}$, $m_2 = -\left[\frac{\eta^S \delta_1^{\,2}\ \rho^F \omega^2 + i\omega\delta_2 \rho^S}{(\eta^F)^2 \rho^S}\right]$, $m_3 = \frac{i\delta_2\ \rho^S}{\delta_1^{\,2}\rho^F\omega + i\delta_2\rho^S}$,

$\bar{m}_1 = -\frac{\bar{\eta}^S}{\bar{\eta}^F}$, $\bar{m}_2 = -\left[\frac{\bar{\eta}^S \bar{\delta}_1^{\,2}\ \bar{\rho}^F \omega^2 + i\omega\delta_2 \bar{\rho}^S}{(\bar{\eta}^F)^2 \bar{\rho}^S}\right]$, $\bar{m}_3 = \frac{i\bar{\delta}_2\ \bar{\rho}^S}{\bar{\delta}_1^{\,2}\bar{\rho}^F\omega + i\bar{\delta}_2\bar{\rho}^S}$.

and A_{01}, B_{01} are amplitudes of the incident longitudinal and transverse waves respectively. A_1, B_1 and $\bar{A}_1$, $\bar{B}_1$ are amplitudes of the corresponding reflected and transmitted waves respectively.

In order to satisfy the boundary conditions, the extension of the Snell's law will be

$$\frac{\sin\theta_0}{V_0} = \frac{\sin\theta_1}{V_1} = \frac{\sin\theta_2}{V_2} = \frac{\sin\bar{\theta}_1}{\bar{V}_1} = \frac{\sin\bar{\theta}_2}{\bar{V}_2}, \tag{32}$$

where

$$k_1 V_1 = k_2 V_2 = \bar{k}_1 \bar{V}_1 = \bar{k}_2 \bar{V}_2 = \omega \text{ at z = 0.} \tag{33}$$

For longitudinal wave,

$$V_0 = V_1, \theta_0 = \theta_1. \tag{34}$$

For transverse wave,

$$V_0 = V_2, \theta_0 = \theta_2. \tag{35}$$

Making the use of potentials given by equations (28) – (31) in boundary conditions (24) –(27) and using the equations (33) - (35), we get a system of four non- homogenous equations which can be written as

$$\sum_{i=1}^{4} a_{ij} Z_j = Y_i, \quad (j = 1,2,3,4), \tag{36}$$

where

$a_{11} = (ik_1 \cos\theta_1)\, l_1$, $a_{12} = (-ik_2 \sin\theta_2)\, l_2$, $a_{13} = (i\bar{k}_1 \cos\bar{\theta}_1)\, l_1 + (r_3 \sin^2\bar{\theta}_1 + r_4 \cos^2\bar{\theta}_1)\bar{k}_1^{\,2}$,

$a_{14} = (i\bar{k}_2 \sin\bar{\theta}_2)\, l_1 + (r_4 - r_3)(\sin\bar{\theta}_2 \cos\bar{\theta}_2)\bar{k}_2^{\,2}$, $a_{21} = (ik_1 \sin\theta_1)\, l_2$, $a_{22} = (ik_2 \cos\theta_2)\, l_2$,

$a_{23} = -(i\bar{k}_1 \sin\bar{\theta}_1)\, l_2 + (-2r_5 \sin\bar{\theta}_1 \cos\bar{\theta}_1)\bar{k}_1^{\,2}$,

$a_{24} = (i\bar{k}_2 \cos\bar{\theta}_2)\, l_2 + r_5(\cos^2\bar{\theta}_2 - \sin^2\bar{\theta}_2)\bar{k}_2^{\,2}$,

$a_{31} = -(r_1 \sin^2\theta_1 + \cos^2\theta_1)k_1^{\,2} - m_2$, $a_{32} = -(r_1 - 1)(\sin\theta_2 \cos\theta_2)k_2^{\,2}$,

$a_{33} = (r_3 \sin^2\bar{\theta}_1 + r_4 \cos^2\bar{\theta}_1)\bar{k}_1^{\,2} + \bar{m}_2$, $a_{34} = (r_4 - r_3)(\sin\bar{\theta}_2 \cos\bar{\theta}_2)\bar{k}_2^{\,2}$,

$a_{41} = (-2r_2 \sin\theta_1 \cos\theta_1)k_1^{\,2}$, $a_{42} = r_2(\sin^2\theta_2 - \cos^2\theta_2)k_2^{\,2}$, $a_{43} = (-2r_5 \sin\bar{\theta}_1 \cos\bar{\theta}_1)\bar{k}_1^{\,2}$,

$a_{44} = r_5(\cos^2\bar{\theta}_2 - \sin^2\bar{\theta}_2)\bar{k}_2^{\,2}$,

and

$r_1 = \frac{\lambda^S}{\lambda^S + 2\mu^S}$, $r_2 = \frac{\mu^S}{\lambda^S + 2\mu^S}$, $r_3 = \frac{\bar{\lambda}^S}{\lambda^S + 2\mu^S}$, $r_4 = \frac{\bar{\lambda}^S + \bar{\mu}^S}{\lambda^S + 2\mu^S}$, $r_5 = \frac{\bar{\mu}^S}{\lambda^S + 2\mu^S}$, $l_1 = r_1 K_n$,

$l_2 = r_1 K_t$, $Z_1 = \frac{A_1}{A^*}$, $Z_2 = \frac{B_1}{A^*}$, $Z_3 = \frac{\bar{A}_1}{A^*}$, $Z_4 = \frac{\bar{B}_1}{A^*}$. (37)

(i) For incident longitudinal wave : $A^* = A_{01}$, $B_{01} = 0$,
$Y_1 = a_{11}$, $Y_2 = -a_{21}$, $Y_3 = -a_{31}$, $Y_4 = a_{41}$.

(ii) For incident transverse wave: $A^* = B_0$, $A_{01} = 0$,
$Y_1 = -a_{12}$, $Y_2 = a_{22}$, $Y_3 = a_{32}$, $Y_4 = -a_{42}$.

where Z_1, Z_2, are amplitude ratio's of reflected longitudinal wave making an angle θ_1 and transverse wave making an angle θ_2 and Z_3, Z_4 are amplitudes ratio's of the transmitted longitudinal wave making an angle $\bar{\theta}_1$ and transmitted transverse wave making an angle $\bar{\theta}_2$ with the normal to the surface.

Case I. Normal stiffness:

$K_n \neq 0$, $K_t \to \infty$ correspond to the case of normal stiffness and we obtain a system of four non- homogenous equations which can be written as given by (36) with the changed values of a_{mn} as:

$a_{31} = (ik_1 \sin\theta_1)$, $a_{32} = (ik_2 \cos\theta_2)$, $a_{33} = -(i\bar{k}_1 \sin\bar{\theta}_1)$, $a_{34} = (i\bar{k}_2 \cos\bar{\theta}_2)$.

Case II. Transverse stiffness:

$K_t \neq 0$, $K_n \to \infty$ correspond to the case of transverse stiffness and we obtain a system of four non- homogenous equations which can be written as given by (36) with the changed values of a_{mn} as

$a_{11} = (ik_1 \cos\theta_1)$, $a_{12} = (-ik_2 \sin\theta_2)$, $a_{13} = (i\bar{k}_1 \cos\bar{\theta}_1)$, $a_{14} = (i\bar{k}_2 \sin\bar{\theta}_2)$.

Case III. Free surface:

$K_t = 0$, $K_n = 0$ correspond to the case of free surface and boundary conditions in this case reduces to

$$T_{33}^{\ S} - p = 0, \tag{38}$$

$$T_{31}^{\ S} = 0, \tag{39}$$

and we obtain a system of two non- homogenous equations which can be written as

$$\sum_{i=1}^{2} a_{ij} Z_j = Y_i, \ (j = 1,2), \tag{40}$$

where a_{11}, a_{12}, a_{21}, a_{22} are given by

$a_{11} = -(r_1 \sin^2\theta_0 + \cos^2\theta_0)k_1^2 - m_2$, $a_{12} = -(r_1 - 1)(\sin\theta_2 \cos\theta_2)k_2^2$,

$a_{21} = (-2r_2 \sin\theta_1 \cos\theta_1)k_1^2$, $a_{22} = r_2(\sin^2\theta_2 - \cos^2\theta_2)k_2^2$.

6. Particular case. Reflection and transmission at the imperfect interface between fluid saturated porous half space and elastic half space

If ρ^F is very small as compare to ρ^S and can be neglected then medium M_2 reduces to elastic half space and we obtain a system of four non- homogenous equations which can be

written as given by (39) with the changed values of a_{mn} as:

$a_{13} = (i\bar{k}_1 \cos\bar{\theta}_1)\, l_1 + (r_6 \sin^2\bar{\theta}_1 + r_7 \cos^2\bar{\theta}_1)\bar{k}_1^2$,

$a_{14} = (i\bar{k}_2 \sin\bar{\theta}_2)\, l_1 + (r_7 - r_6)(\sin\bar{\theta}_2 \cos\bar{\theta}_2)\bar{k}_2^2$,

$a_{23} = -(i\bar{k}_1 \sin\bar{\theta}_1)\, l_2 + (-2r_8 \sin\bar{\theta}_1 \cos\bar{\theta}_1)\bar{k}_1^2$,

$a_{24} = (i\bar{k}_2 \cos\bar{\theta}_2)\, l_2 + r_8(\cos^2\bar{\theta}_2 - \sin^2\bar{\theta}_2)\bar{k}_2^2$,

$a_{33} = (r_6 \sin^2\bar{\theta}_1 + r_7 \cos^2\bar{\theta}_1)\bar{k}_1^2$, $a_{34} = (r_7 - r_6)(\sin\bar{\theta}_2 \cos\bar{\theta}_2)\bar{k}_2^2$,

$a_{43} = (-2r_8 \sin\bar{\theta}_1 \cos\bar{\theta}_1)\bar{k}_1^2$, $a_{44} = r_8(\cos^2\bar{\theta}_2 - \sin^2\bar{\theta}_2)\bar{k}_2^2$,

$r_6 = \dfrac{\bar{\lambda}^e}{\lambda^S + 2\mu^S}$, $r_7 = \dfrac{\bar{\lambda}^e + \bar{\mu}^e}{\lambda^S + 2\mu^S}$, $r_8 = \dfrac{\bar{\mu}^e}{\lambda^S + 2\mu^S}$.

7. Numerical results and discussion

With the view of illustrating the theoretical results and for numerical discussion we take a model for which the values of the various physical parameters are taken from De Boer and Ehlers [10] as follows:

$\eta^S = 0.67$, $\eta^F = 0.33$, $\rho^S = 1.34\ \text{Mg}/m^3$, $\rho^F = 0.33\ \text{Mg}/m^3$,

$\lambda^S = 5.5833\ \text{MN}/m^2$, $K^F = 0.01\text{m/s}$, $\gamma^{FR} = 10.00\text{KN}/m^3$, $\mu^S = 8.3750\ \text{MN}/m^2$,

$\bar{\eta}^S = 0.6$, $\bar{\eta}^F = 0.4$, $\bar{\rho}^S = 2.0\ \text{Mg}/m^3$, $\bar{\rho}^F = 0.01\ \text{Mg}/m^3$, $\bar{\lambda}^S = 4.2368\ \text{MN}/m^2$,

$\bar{K}^F = 0.02\ \text{m/s}$, $\bar{\gamma}^{FR} = 9.00\text{KN}/m^3$, $\bar{\mu}^S = 3.3272\ \text{MN}/m^2$, $\bar{\rho}^e = 2.65\text{Mg}/m^3$,

$\bar{\lambda}^e = 2.238\ \text{MN}/m^2$, $\bar{\mu}^e = 2.238\ \text{MN}/m^2$.

A computer program has been developed and amplitude ratios of various reflected and transmitted waves has been computed. The variations of amplitude ratios for fluid saturated porous half spaces with stiffness (ST), with normal stiffness (NS) and with tangential stiffness (TS) have been shown by solid line, long dashed line and small dashed lines respectively. Solid lines without central symbols correspond to the case of fluid saturated porous half space (FS) whereas Solid lines with central symbols correspond to the case of elastic half space (ES).

The variations of amplitude ratios $|Z_i|$ (i = 1, 2, 3, 4) for ST, NS, and TS with angle of incidence for longitudinal wave (LW) and transverse wave (TW) are shown graphically in Figs. 1-8. Figures 9 -12 show the variations of amplitude ratios $|Z_i|$ (i = 1, 2) for longitudinal waves (LW) and transverse waves (TW) at the free surface .

7.1. Incident longitudinal wave. The values of amplitude ratios $|Z_1|$ in case of ES are more than the values for FS in all the three cases of ST, NS and TS in the range $0^0 \le \theta^0 \le 90^0$. Its values in case of FS increase in the range $0^0 \le \theta^0 \le 13^0$, $28^0 \le \theta^0 \le 35^0$, $38^0 \le \theta^0 \le 90^0$ and decrease in the remaining range for ST and NS whereas its values decrease in the range $0^0 \le \theta^0 \le 13^0$, $33^0 \le \theta^0 \le 45^0$ and increase in the remaining range for TS. These variations are shown in Fig. 2.

The variations of amplitude ratios $|Z_2|$ are shown in Fig. 3. The values of amplitude ratios $|Z_2|$ in case of ES are less than the values of FS in all the three cases of ST, NS and TS in the

whole range $0^0 \leq \theta^0 \leq 90^0$.

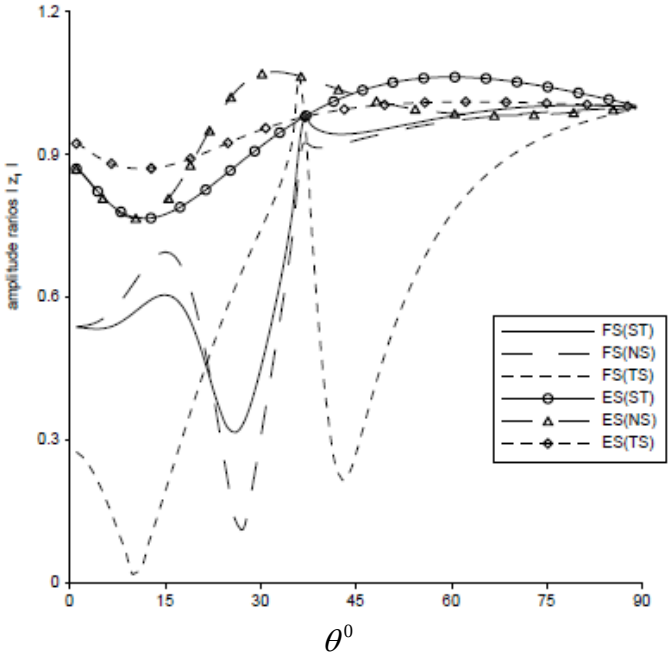

Fig. 2. Variation of amplitude ratios $|Z_1|$ with angle of incidence for longitudinal wave.

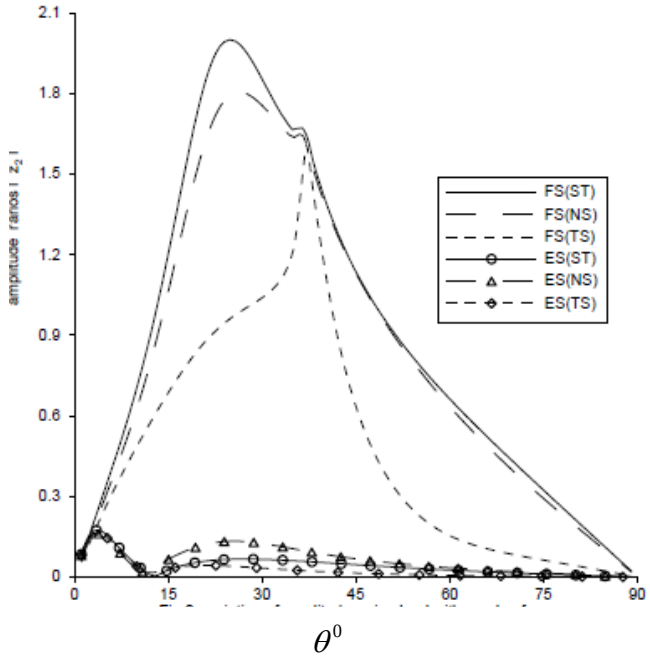

Fig. 3. Variation of amplitude ratios $|Z_2|$ with angle of incidence for longitudinal wave.

Figure 4 depicts the behavior of variations of amplitude ratios $|Z_3|$ for FS and ES. Values of amplitude ratios $|Z_3|$ for TS boundary are less than for ST and NS in both the cases FS and ES. The values of amplitude ratios $|Z_3|$ in case of ES are more than the values of FS for ST and NS in the whole range $0^0 \leq \theta^0 \leq 90^0$ whereas in case TS these values are more in the range $0^0 \leq \theta^0 \leq 43^0$ and less in the range $43^0 \leq \theta^0 \leq 90^0$.

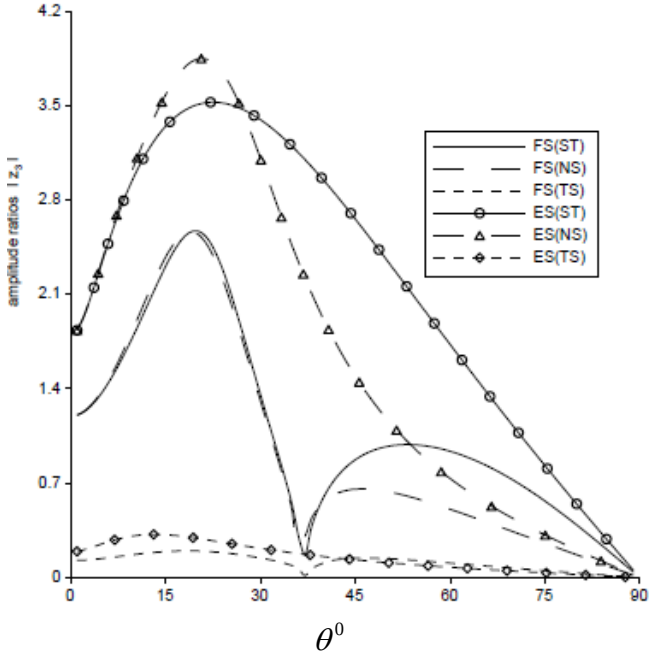

Fig. 4. Variation of amplitude ratios $|Z_3|$ with angle of incidence for longitudinal wave.

The values of amplitude ratios $|Z_4|$ for FS increase in the range $0^0 \le \theta^0 \le 23^0$, $37^0 \le \theta^0 \le 50^0$ and decrease in the remaining range. The values of amplitude ratios $|Z_4|$ in case of ES increase in the range $0^0 \le \theta^0 \le 20^0$ then decrease in the remaining range. These variations are shown in Fig. 5.

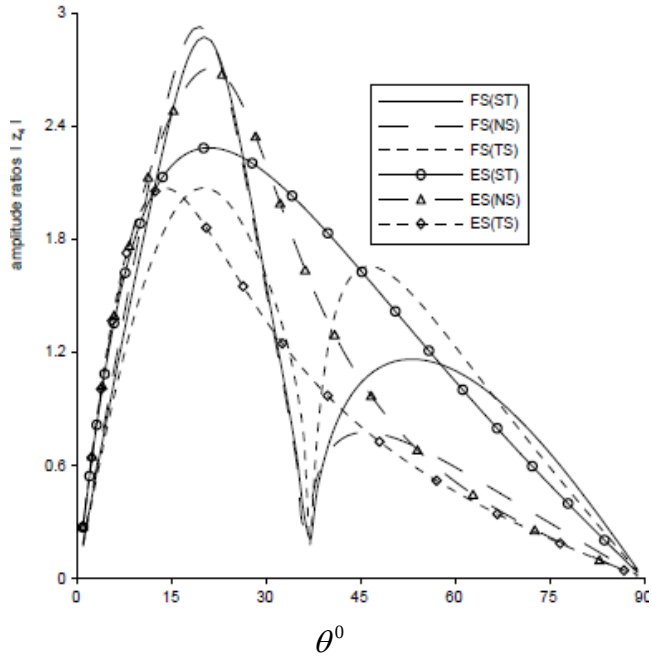

Fig. 5. Variation of amplitude ratios $|Z_4|$ with angle of incidence for longitudinal wave.

7.2. Incident transverse wave. The values of amplitude ratios $|Z_1|$ in case of FS have an oscillatory behavior for TS in the whole range $0^0 \le \theta^0 \le 90^0$ and increase in the whole range for

ST and NS. The values of amplitude ratios $|Z_1|$ in case of ES increase in the whole range for TS and these values increase for ST and NS except in the range $30^0 \leq \theta^0 \leq 35^0$. These variations are shown in Fig. 6.

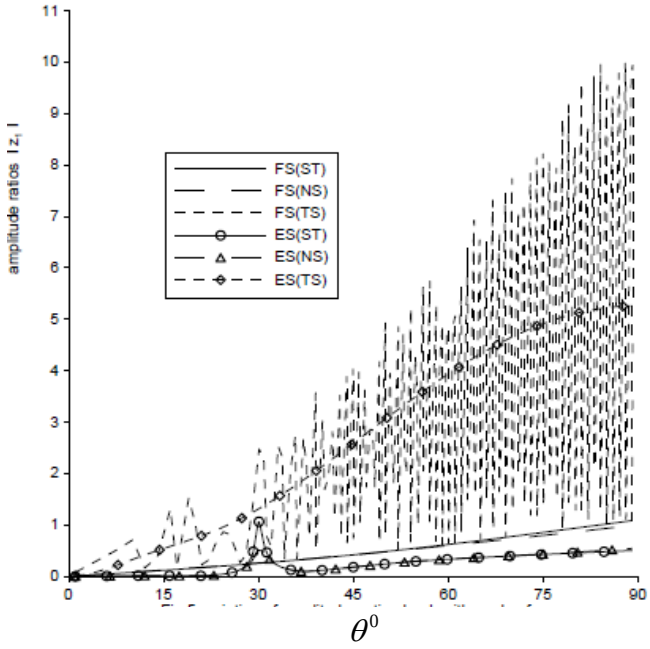

Fig. 6. Variation of amplitude ratios $|Z_1|$ with angle of incidence for transverse wave.

It is evident from Fig. 7 that values of amplitude ratios $|Z_2|$ in case of FS increase gradually in the whole range $0^0 \leq \theta^0 \leq 90^0$. The values of amplitude ratios $|Z_2|$ in case of ES decrease in the range $0^0 \leq \theta^0 \leq 20^0$, $32^0 \leq \theta^0 \leq 40^0$ and increase in the remaining range for ST and NS whereas these values increase in the whole range for TS.

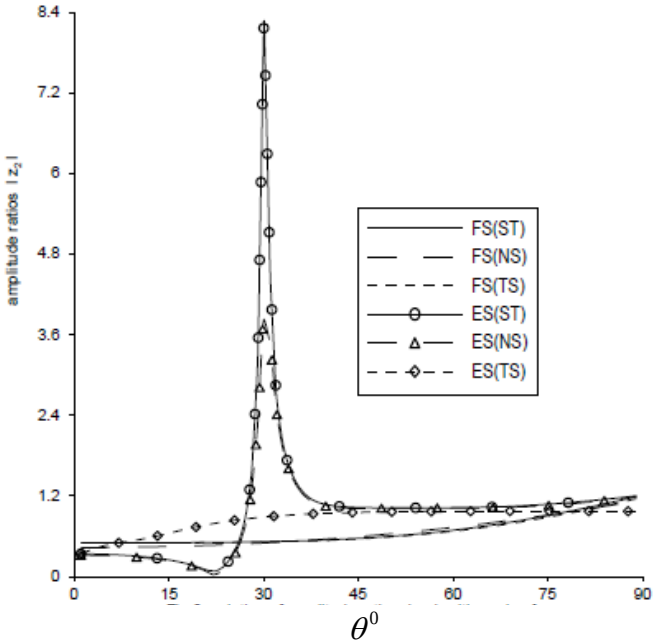

Fig. 7. Variation of amplitude ratios $|Z_2|$ with angle of incidence for transverse wave.

The values of amplitude ratios $|Z_3|$ in case of ES decrease in the range $30^0 \leq \theta^0 \leq 35^0$ and increase in the remaining range for ST, NS and these values increase in the range $0^0 \leq \theta^0 \leq 45^0$ and decrease in the range $45^0 \leq \theta^0 \leq 90^0$ for TS. The values of amplitude ratios $|Z_3|$ in case of FS have an oscillatory behavior for TS in the range $0^0 \leq \theta^0 \leq 90^0$ and increase in the whole range for ST and NS. These variations are shown in Fig. 8.

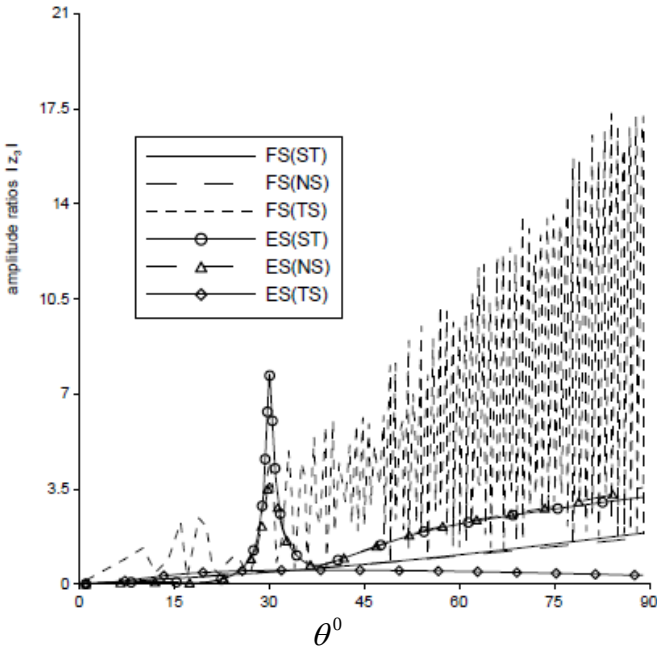

Fig. 8. Variation of amplitude ratios $|Z_3|$ with angle of incidence for transverse wave.

Figure 9 shows that the values of amplitude ratios $|Z_4|$ for FS are close to each other in all three cases of ST, NS and TS whereas for ES these values in case of TS are more than the values of ST and NS.

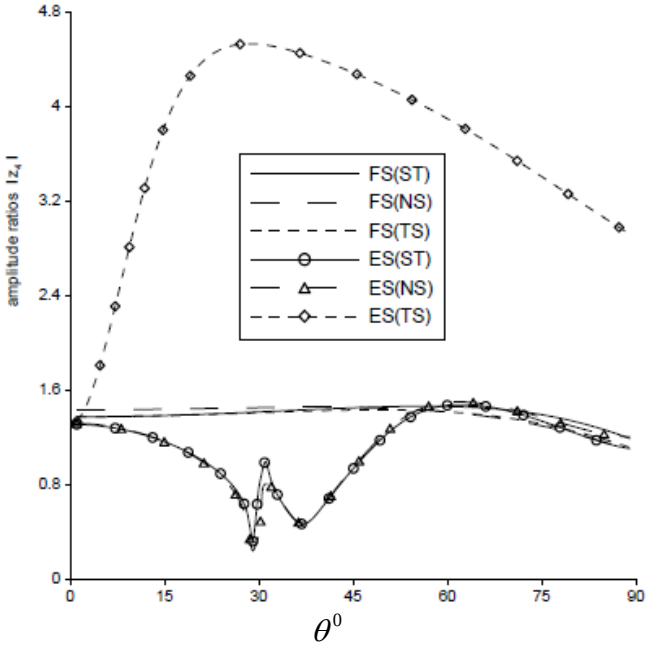

Fig. 9. Variation of amplitude ratios $|Z_4|$ with angle of incidence for transverse wave.

7.3. Incident longitudinal wave at the free surface. Figure 10 depicts the behavior of variations of amplitude ratios $|Z_1|$ for FS and ES. Values of amplitude ratios in case of FS increase in the range $0^0 \le \theta^0 \le 37^0$, $60^0 \le \theta^0 \le 90^0$ and decrease in the remaining range. The values of amplitude ratios $|Z_1|$ in case of ES are constant in the whole range $0^0 \le \theta^0 \le 90^0$.

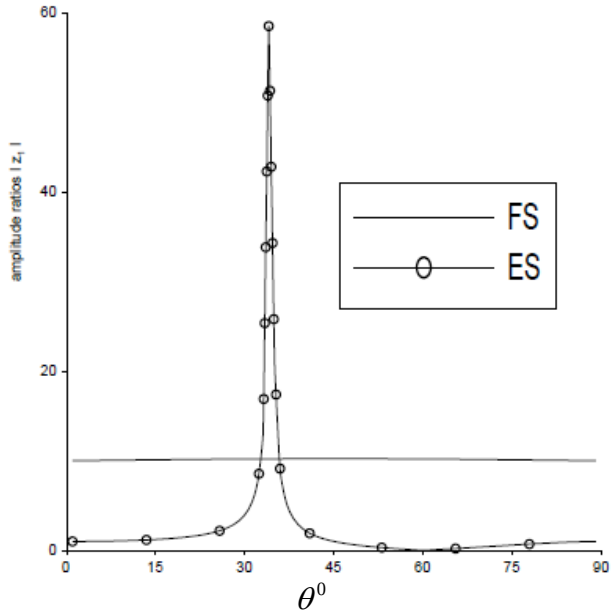

Fig. 10. Variation of amplitude ratios $|Z_1|$ with angle of incidence for longitudinal wave at the free surface $z = 0$.

It is noticed from Fig. 11 that values of amplitude ratios $|Z_2|$ in case of ES start with small initial increase and oscillates in the range $30^0 \le \theta^0 \le 35^0$ and decrease slowly in the remaining range. The values of amplitude ratios $|Z_2|$ in case of FS decrease sharply in the range $0^0 \le \theta^0 \le 15^0$ and then decrease slowly in the remaining range.

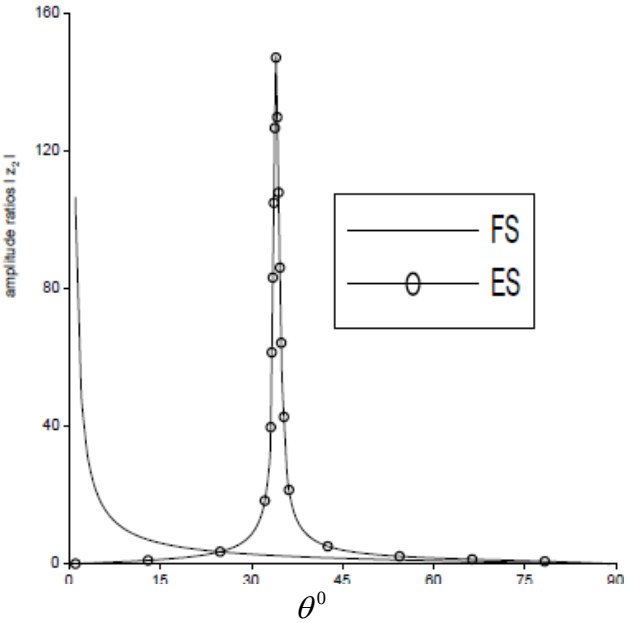

Fig. 11. Variation of amplitude ratios $|Z_2|$ with angle of incidence for longitudinal wave at the free surface $z = 0$.

7.4 Incident transverse wave at the free surface. Figure 12 shows that the values of amplitude ratios $|Z_1|$ for ES start with small initial increase then oscillate in the range $15^0 \le \theta^0 \le 20^0$ and $35^0 \le \theta^0 \le 43^0$ and decrease slowly in the remaining range whereas for FS its values increase monotonically in the whole range.

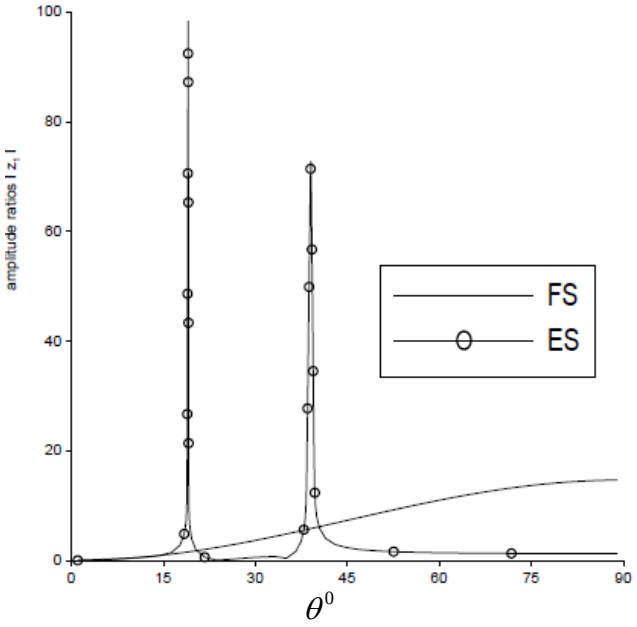

Fig. 12. Variations of amplitude ratios $|Z_1|$ with angle of incidence for transverse wave at the free surface $z = 0$.

It is observed from Fig. 13 that values of amplitude ratios $|Z_2|$ in case of FS oscillates about the value zero in the whole range $0^0 \le \theta^0 \le 90^0$ whereas for ES its values start with small initial increase then oscillate in the range $15^0 \le \theta^0 \le 19^0$ and $40^0 \le \theta^0 \le 42^0$ and decrease slowly in the remaining range .

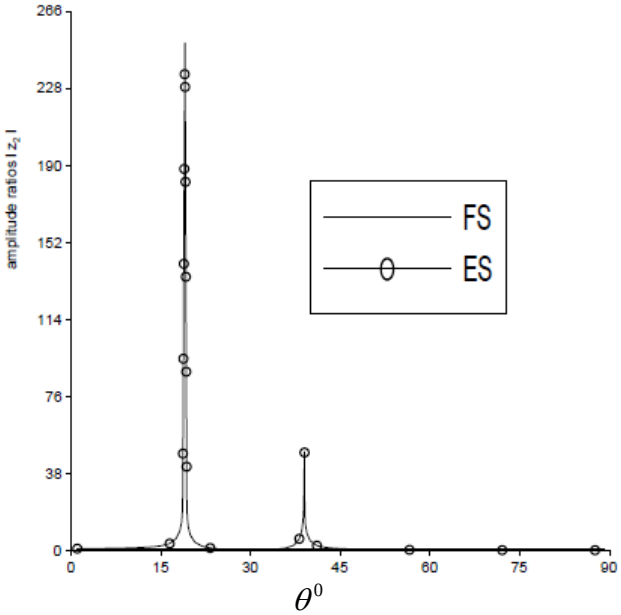

Fig. 13. Variations of amplitude ratios $|Z_2|$ with angle of incidence for transverse wave at the free surface $z = 0$.

8. Conclusions

The analytic expressions of the amplitude ratios for various reflected and transmitted waves are obtained for an imperfect boundary between two different fluid saturated porous half spaces. Different types of special cases have been deduced and discussed. It is concluded that imperfect boundary and porosity have significant effect on amplitude ratios. The model presented in this paper is one of the more realistic forms of the earth models. It may be of some use in seismology, engineering and geophysics etc.

References

[1] K. Von Terzaghi // Sitzungsber Akad. Wiss. (Wien), Math. – Naturwiss. Kl, Abt. IIa **132** (1923) 125.

[2] K. Von Terzaghi, *Erdbaumechanik auf Bodenphysikalischer Grundlage* (Franz Deuticke, Leipzig – Wien, 1925).

[3] M.A. Biot // *J. Appl. Phys.* **12**, Iss. 2 (1941) 144.

[4] M.A. Biot // *J. Acoust. Soc. Am.* **28** (1956a) 168.

[5] M.A. Biot // *J. Acoust. Soc. Am.* **28** (1956b) 179.

[6] P. Fillunger // *Osterr. Wochenschrift fur den Offent. Baudienst*. Teile **I-III** (1913) 532.

[7] R.M. Bowen // *J. Int. J. Eng. Sci.* **18** (1980) 1129.

[8] R. De Boer, W. Ehlers // *Acta Mechanica* **83** (1990) 77.

[9] R. De Boer, W. Ehlers // *Int. J. Solids Struct.* **26** (1990) 43.

[10] R. De Boer, W. Ehlers, Zh. Liu // *Arch. App. Mech.* **63** (1993) 59.

[11] R. Kumar, B.S. Hundal, In: *Currents Trends in Industrial and Applied* Mathematics, ed. by P. Manchanda, K. Ahmad, A.H. Siddiqi (Anamya Publishers, New Delhi, 2002), p. 181.

[12] R. Kumar, B.S. Hundal // *Indian J. Pure and Applied Math*. **4** (2003) 51.

[13] R. Kumar, B.S. Hundal // *Bull. Allahabad Math. Soc.* 18 (2003) 1.

[14] R. Kumar, B.S. Hundal // *Bull .Cal. Math. Soc.* **96 (3)** (2004) 179.

[15] R. Kumar, B.S. Hundal // *J. of Sound and Vibration* **288** (2005) 361.

[16] H. Deresiewicz // *Bull. Seismol. Soc. Am.* **50** (1960) 599.

[17] P. Malla Reddy, M. Tajuddin // *Int. J. Solids Struct.* **37** (2000) 3439.

[18] R. Kumar, S. Deswal // *Indian J. Pure Appl. Math.* **31(10)** (2000) 1317.

[19] S.K. Tomar, Jaswant Singh // *Applied Mathematics and Computation* **169** (2005) 671.

[20] S.K. Tomar, Ashish Arora // *Int. J. Solids Struct.* **43** (2006) 1991.

[21] M. Tajuddin, S.J. Hussaini // *Journal of Applied Geophysics* **58** (2006) 59.

[22] J.P. Jones, J.S. Whittier // *J. Appl. Mech.* **34** (1967) 905.

[23] G.S. Murthy // *Phys. Earth and Planetary Interiors* **11** (1975) 65.

[24] A.H. Nayfeh, E.M. Nassar // *J. Appl. Mech.* **45** (1978) 822.

[25] S.I. Rokhlin, M. Hefets, M. Rosen // *J. Appl. Phys.* **51** (1980) 3579.

[26] S.I. Rokhlin, In: *Adhesive Joints: Formulation, Characteristics and Testing*, ed. by K.L. Mittal (Plenum, New York, 1984), p. 307.